Silicon (2015) 7:283–291
DOI 10.1007/s12633-014-9227-x

ORIGINAL PAPER

Investigation of Novel Silicon PV Cells of a Lateral Type

A. Axelevitch · V. Palankovski · S. Selberherr · G. Golan

Received: 29 July 2013 / Accepted: 28 July 2014 / Published online: 20 August 2014

Abstract Solar cells made of single-crystalline silicon, as alternative energy sources, became the most widely used solar cells in recent years. The mainstream manufacturing approach is to process the cells and assemble these into photovoltaic (PV) modules. However, the direct conversion of solar energy into electricity using the PV effect suffers from low efficiency. Thus, increasing the conversion efficiency at low production costs becomes the main goal of solar cell manufacturers. One way to increase the efficiency of a solar cell is to use an ultra-wide layer of intrinsic semiconductor as the depletion region of a PN junction. In our work, we present a novel geometrical concept of PIN structure for PV applications. The width of the intrinsic layer in our construction is 5-20 mm. Moreover, in our novel structure, the light irradiation acts directly on the active region of the PV cell, which enables bi-facial irradiation and results in ∼28 % conversion efficiency. A low cost fabrication is ensured in our design due to a new manufacturing technology by eliminating some expensive processes, such as photolithography. The feasibility proof of the novel concept in mono-crystalline silicon solar cells is presented. We demonstrate simulation results and preliminary experimental results confirming our approach.

A. Axelevitch (✉) · G. Golan
Holon Institute of Technology (HIT), 52 Golomb Str., 5810201, Holon, Israel
e-mail: alex_a@hit.ac.il

V. Palankovski · S. Selberherr
Institute for Microelectronics, TU Wien, Gußhausstraße, 1040, Vienna, Austria

Keywords Single-crystalline silicon · PIN structure · Lateral PV cell · Simulation

1 Introduction

Solar cells, as an alternative energy source, attracted much attention in the last decades. The sun represents an energy source which sends to earth enormous energy. It is known that the solar power obtained on earth is about 1.2×10^{17} W. The maximum theoretical efficiency of solar light to electricity conversion may reach ∼93 % [1]. Thus, solar cells have a real potential to replace fossil fuels as the main means of electric power generation. However, existing solar cells suffer from two main deficiencies: relatively low efficiency, and high cost in comparison with conventional fossil fuel electric sources. Thus, there are significant reasons to put efforts and resources to develop low-cost highly-efficient PV converters.

Almost 90 % of all produced solar cells were made of single and polycrystalline silicon. Single crystalline silicon solar cells are the most widely used today. Together with the polycrystalline cells, which are slightly less efficient, they represent the base line of today's market. At the same time, thin film solar cells made of amorphous silicon (a-Si) became significant in the commercial photovoltaic device market. Unfortunately, solar cells made by chemical vapor deposition (CVD) methods suffer low efficiency and significant degradation under solar irradiation (the Staebler-Wronski effect). Also, due to the small thickness of the semiconductor layers, a substantial part of the solar light cannot be absorbed (photons with wavelength above 800 nm).

Efficiency of energy conversion in practical solar cells is limited by losses caused by electrical, optical, and technological reasons. The spectral sensitivity of various semiconductors has a significant contribution to the optical losses. All photons with energy lower than the semiconductor bandgap cannot generate electron-hole pairs and thus are lost. Photons with energy that is higher than the bandgap generate charged carriers which transfer additional energy to the semiconductor material (the thermalization process) and heat up the photovoltaic device. This increasing heat decreases the cell's efficiency. Metal contacts (fingers and busbars), located on the active surface of the solar cell (see Fig. 1) reduce the area that absorbs light (by ∼20 %), which leads to losses (∼10 % for optimized patterns [2]). Different approaches for reduction of these losses have been sought, e.g., by using rear-side contacts only [3] or using electrically-conductive optically-transparent materials [4].

Electrical losses significantly affect both the current and the voltage of a solar cell. These losses may be conditionally divided into two major groups: losses due to the electrical transport (Ohmic losses) and recombination losses given by various recombination mechanisms. The Ohmic losses consist of electrical resistance to transport of charged carriers within the doped regions of the device: emitter and base, resistance of the PN junction, contact resistances on the borders of the semiconductor and metal collectors, and the resistance of thin metal films of the busbars system. The recombination losses are defined by various processes in the semiconductor: radiative recombination (luminescence), Auger recombination, recombination on the semiconductor defects and impurities (Shockley-Read-Hall or SRH recombination), and surface recombination, see e.g. [6, 7].

Technological losses are made up of various inaccuracies and incompatibilities at each stage of the technological process. These losses are determined by a plurality of different independent factors, incorrect selection of which can lead to complete failure of solar cells. Consequently, the appropriate technology must take into account all possible mechanisms of losses and reduce the influence of each one of them.

Fig. 1 External view of a conventional solar cell [5]

2 PIN Structure Performance

The space charge region takes a small part of the effective zone in conventional PN diode type PV solar cells. However, the generated current can be increased by widening the space charge region. This may be achieved by introducing additional intrinsic (I-) semiconductor layer between the P and N parts of the diode (PIN structure). The main difference between the PN diode and the PIN diode is that the internal electric field is limited to the depletion layer in the PN-type diode, whereas it extends over the whole I-layer in the PIN-type diode [8].

The operating principle of photovoltaic solar cells is generation of charged carriers under irradiation and their separation by the internal built-in electric field. So, the location of this electric field and its value are most significant. Generally, the travel distance from the origin point to the suitable electrode is determined by the carrier diffusion length. Maximum value of this parameter may reach the order of 1 cm for the single-crystalline Si or Ge [9]. In the case of a PIN-diode structure, collection of the charged carriers is governed by the drift length of both electrons and holes within the intrinsic layer. It can be shown that, under "reasonable conditions", the drift value is a few times larger than the minority carrier diffusion length [10]. Thus, if the quality of the applied material is high, highly-efficient PIN solar cells based on single-crystalline silicon may be achieved.

3 Novel Construction of the Solar Cell

All types of conventional solar cells have one common property: photons penetrating the front surface of the cells generate electrons and holes which move in the direction of photons (holes) and in opposite direction (electrons). Such conventional systems are designated as "vertical behaving" systems. We turn this construction so that charged particles begin to move perpendicular to the direction of the incoming photons. We also widen the intrinsic zone and make emitter and base significantly thinner. A cross-section of such a novel PIN construction of the PV cell is presented in Fig. 2.

This PV cell represents a single-crystalline silicon strip, ∼10 mm wide and 10 cm long, having the maximal surface area of 10 cm^2 oriented in [001] direction. It is grown as pure single crystal material having an intrinsic concentration of charged carriers. The strip is heavily doped by donors at one side ($N_D \approx 10^{19} cm^{-3}$) and by acceptors at the other side ($N_A \approx 10^{19} cm^{-3}$). Both sides are also coated by metal

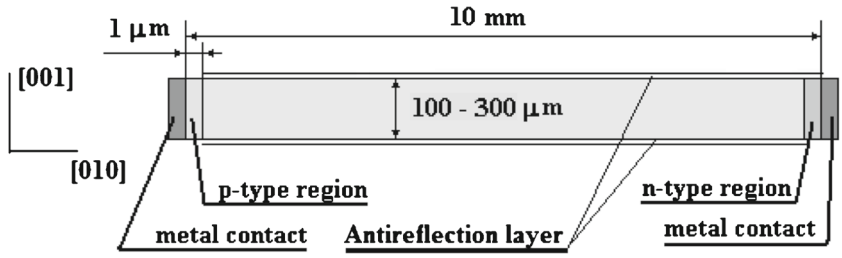

Fig. 2 Novel PIN construction of the PV cell

Ohmic contacts. The front and rear surfaces of the cell are coated by anti-reflection coating. Figure 3 shows approximately the net charge distribution in the novel cell (Fig. 3c), the electric field distribution (Fig. 3d), and the travel directions of incoming photons and generated charged carriers (Fig. 3a). This structure may be designated as a "lateral PV cell" due to the perpendicular direction of charged carriers moving relative to the photons incoming.

As can be seen, almost the entire surface of the PV cell is active and absorbs photons. This wide active intrinsic zone is completely undoped. Consequently, the mean free path of the charged carriers and their mobility reaches its maximum value. The SRH recombination is negligibly low. Since the main mechanism of separation of the generated charged carriers is the internal built-in electric field, it is interesting to calculate its value and its spatial distribution to achieve complete charge separation in this novel system.

Using a simple model of depletion zones [11], the calculated constant electric field in the intrinsic region is very high ($\sim 10^6$ V/cm) and the voltage, generated by this cell is 10^6 V. On the other hand, this voltage is approximately equal to the sum of the two built-in potentials, generated at the junctions, i.e. ~1V! This contradiction suggests that the depletion model does not describe the junctions (P+/I and N+/I) correctly. Moreover, the built-in electric field cannot be constant inside the depletion zone. To find the correct description of the PIN structure, we must consider the physical processes at the P+/I and N+/I junctions in detail.

The full-depletion approximation assumes that the depletion region around the metallurgical junctions has well-defined edges [12]. It also assumes that the transition between the depletion region and the quasi-neutral region is abrupt. Here, the quasi-neutral region is defined as the region adjacent to the depletion region. In the quasi-neutral region, the electric field is small and the free carrier density is close to the net doping density.

The PV cell shown in Fig. 3 has abruptly doped sides that may be realized simply enough, for example by an epitaxial growth process. However, the depletion regions close to the quasi-neutral sides are not free of mobile charged carriers. There is a dynamic steady-state process. Therefore, for analysis of this device we must use the Poisson equation together with the current continuity equations for electrons and holes (drift-diffusion transport model) [13].

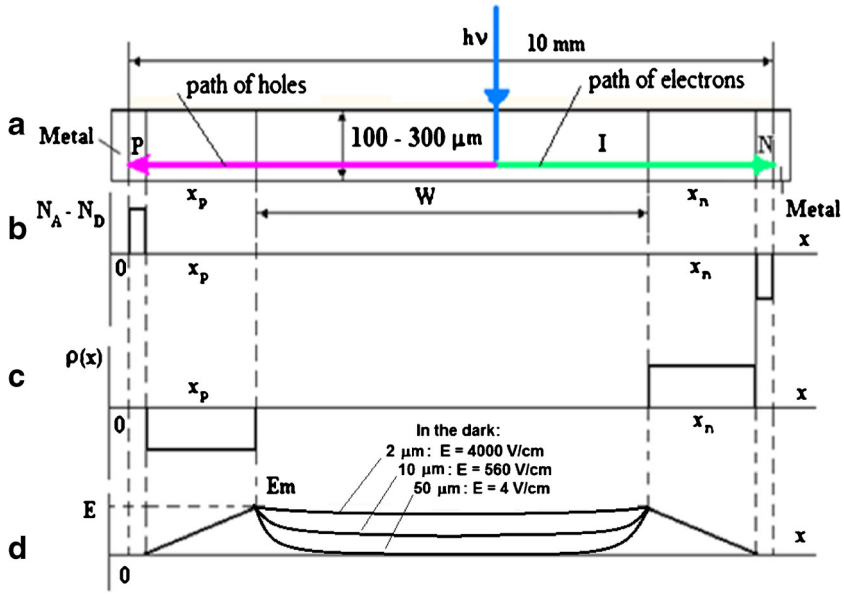

Fig. 3 A cross-section view of the novel solar element

4 Simulation

Simulation of the novel type PV cell must answer a series of questions:

1 What is the distribution of the built-in electric field in the lateral PIN structure?
2 Which mechanism drives charged carriers in this structure?
3 What efficiency may be reached in the lateral PIN structure?
4 Bi-facial irradiation – possibility to application.
5 Evaluation of the influence of various technological factors and external conditions on the basic PV cells' parameters (open circuit voltage, short circuit current, efficiency).

In order to check the distribution of the built-in electric field at the junction between the side electrode and the intrinsic region, numerical simulation of the abrupt PIN diode structure with the width W =5 mm and the thickness D = 200μm was performed under equilibrium in dark conditions. At the side electrodes, doping concentrations $N_D = N_A = 10^{19}$ cm^{-3} were selected.

Figure 4 presents the simulated electric field and electrostatic potential along a lateral cross-section within the PI transition zone. The concentration value in the intrinsic zone was chosen at the ν-level ($N_D \approx 10^{12}$ cm^{-3}). This simulation was performed using the ATLAS device simulator [14], which solves the fundamental semiconductor equations numerically. The simulation results show that the electric field is not constant within the transition zone. A large concentration of holes existing in the zone close to the metallurgical abrupt junction defines the electric field behavior. The electric field reaches thousands and tens of thousands volts per centimeter for sufficiently small sizes (up to 2 μm), drops to hundreds V/cm when the length increases to 5 μm, becomes insignificant at 10 μm, and disappears for large values of the region length, as shown in Fig. 3d [15]. This is in contradiction with the analytical model based on the depletion approximation. So, we cannot assume that this zone, close to the junction, is depleted. Therefore, estimation of the built-in electric field within the I-region breaks down and the electric field cannot be constant therein.

However, the irradiation drastically changes this picture. Figure 5 presents the simulation results for PV behavior under irradiation with various light intensities. This simulation was provided for a sample having doping concentrations on both sides $N_D = N_A = 10^{19}$cm^{-3} and a width W = 1mm. In this experiment, the sample coated by an antireflection thin film was illuminated by monochromatic light with a wavelength of 800 nm from one side. The antireflection layer thickness was 70 nm. The Minimos-NT device simulator suitable for simulation of solar cells [16] was used.

In this simulation, no contact resistance was considered. However, SRH bulk and surface recombination are accounted for. Carrier lifetimes of 0.1 ms and surface recombination velocity at the front side of 1000 cm/s are assumed. As shown in Fig. 5, our novel PV cell construction generates electricity according to the received light energy. Also, as shown in Fig. 2, this construction of a PV cell enables bi-facial illumination since it has two active surfaces: front and rear. Simulation of bi-facial illumination shows a double growth of electricity generated. In order to clarify what mechanism is responsible for the charge separation in the cell, the simulation of electric fields in both cases: dark and under illumination, was performed. Figure 6 compares the electric field in a 1 mm width cell with and without irradiation at zero bias.

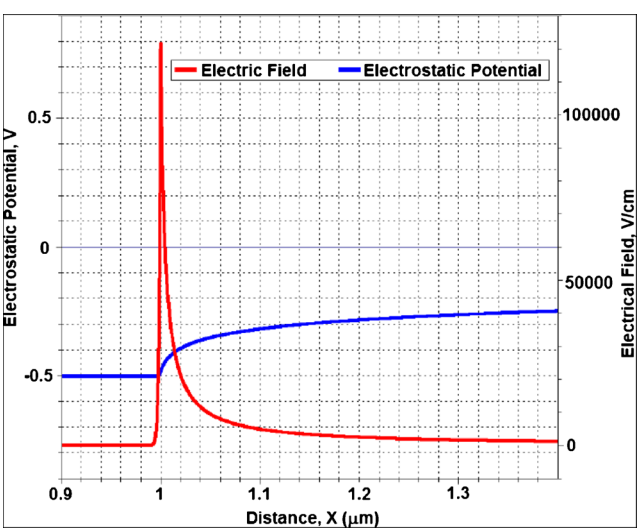

Fig. 4 Electric field and electrostatic potential at the PI junction of the lateral PIN structure

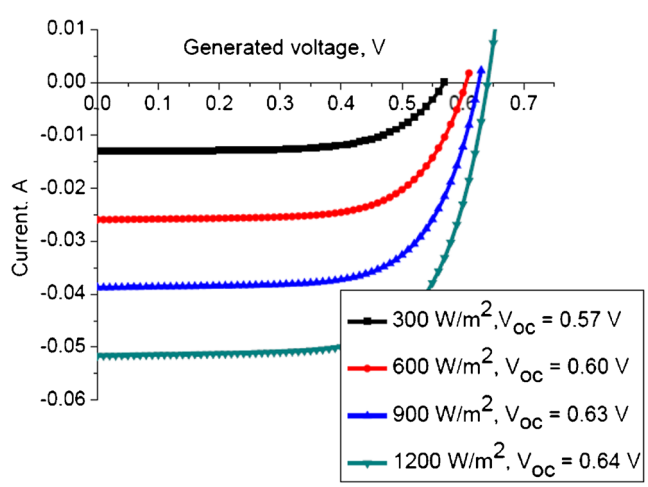

Fig. 5 I-V characteristics for various light intensities

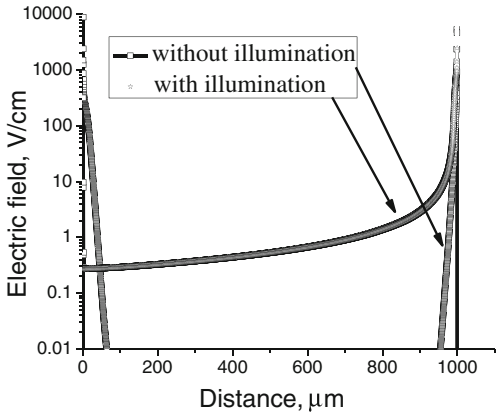

Fig. 6 Electric field along the cell width

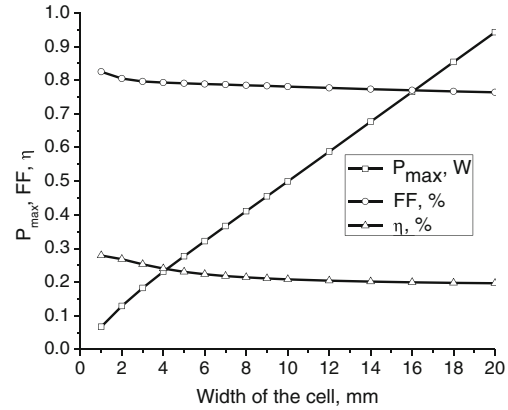

Fig. 8 Maximum power, fill factor, and efficiency vs. cell width

As shown, the electric field looks different in the two simulated cases. In the case of darkness, there is a high electric field near the contact. This field reaches 30 kV/cm and drops very quickly with the distance. This picture dramatically changes with illumination. Now, the field is able to separate the charges and transfer them to the electrodes. In this case, the dominant transport mechanism is a drift caused by the electric field.

Figure 7 presents simulation of the cell behavior with different trap concentrations under bi-facial illumination. The trap concentration value $N_t = 10^{12}$ cm^{-3}, resulting in carrier lifetimes of ~0.1 ms, is very high for intrinsic silicon. If we decrease the trap concentration to $N_t = 10^{10}$ cm^{-3}, corresponding to lifetimes of ~10 ms, or simulate the cell behavior without SRH recombination, we obtain a significant increase of I_{sc} and V_{oc}. As shown in Fig. 7, the number of traps (crystal defects, impurities, etc.) in silicon strongly affects its transport properties. Therefore, the silicon must be pure, single crystalline, and properly positioned for PV cell preparation.

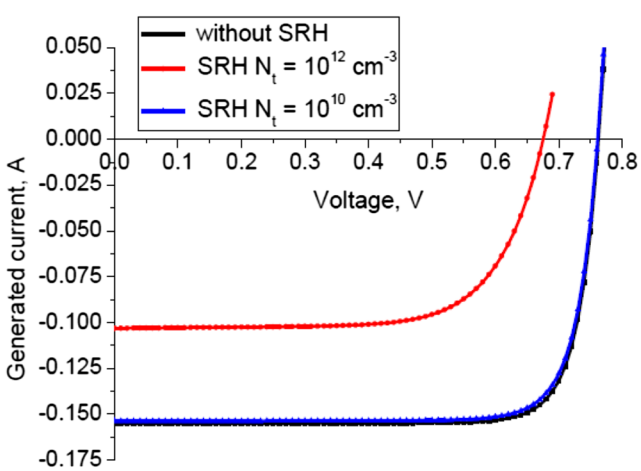

Fig. 7 I-V characteristics for various SRH recombination

The behavior of the novel PV cell depends on the ambient temperature as that of the conventional vertical cells. For silicon the theoretical estimation [2] gives a reduction in the open circuit voltage V_{oc} of about 2.3 mV/K. Our simulation results at various ambient temperatures between 300 K and 400 K show that, while the short circuit current I_{sc} remains nearly the same, V_{oc} decreases with reduction of ~2 mV/K.

All of the above simulations were performed for a cell's width of W = 1 mm. However, the real cell's width should be higher. Figure 8 presents the maximum generated power (P_{max}, W), fill factor (FF, %), and efficiency (η, %) as functions of the cell's width. These simulations were based on illumination according to the ASTM G173-03 reference spectra, which gives after integration 832 W/m^2 power intensity for the range: λ = 400-1000 nm and for integral solar power intensity of 1200 W/m^2. The generated electricity grows proportionally to the received solar power. Evidently, electricity losses also grow together with the width increase.

As can be seen from the graphs, the maximum efficiency reaches 28 % for narrow cells and slightly less for wider cells. The results of these simulations give evidence for

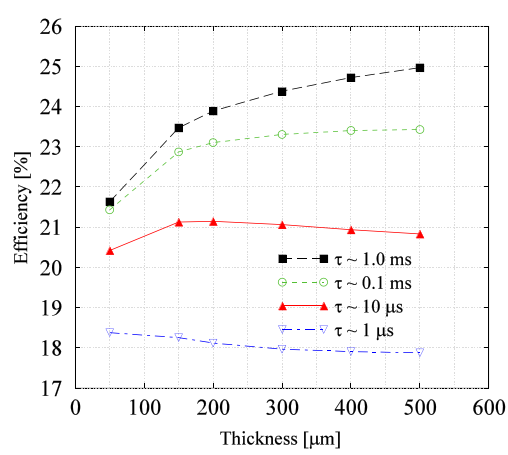

Fig. 9 Projected efficiency as a function of the vertical cell thickness

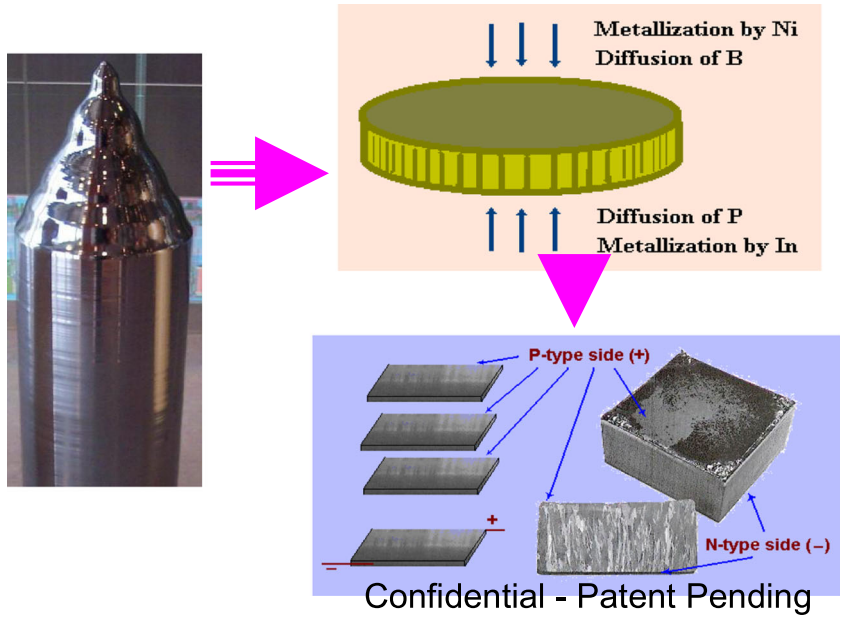

Fig. 10 Straight forward technology for the novel PV cell fabrication [17]

achieving high efficiencies with our novel PV cells in lateral mode of operation.

We have actually compared by means of two-dimensional numerical simulation conventional vertical silicon thin film solar cells (see Fig. 9) using the same simulator and exactly the same models and model parameters. The figure shows the projected efficiencies as a function of the cell's thickness with carrier lifetime as a parameter. As can be seen, our lateral structure has the potential to deliver higher efficiencies (28 % vs. 22 %-25 %).

5 Experimental Implementation

The feasibility proof of our novel PV cell was based on the patent application of Golan et al. [17]. Figure 10 presents the straight forward technology based on this patent application.

However, in practical implementation of the new PV cells we had some technological difficulties. Almost all globally manufactured single-crystalline silicon is of P-type, due to the requirements of the microelectronics industry as the major player on the silicon market. Thus, the silicon which was used in our experiments was of P-type with resistivity of $\sim$10 kΩ·cm, which corresponds to an acceptor concentration of $\sim 10^{13}$ cm^{-3}. This is a possible reason for increased recombination and, consequently, electrical losses, compared to those in intrinsic material. Also, we had to use silicon wafers with thickness of 200-300 μm instead of thick silicon crystals. Therefore, instead of the straight forward technology we have applied another technology illustrated with Fig. 11.

This technology involves the use of standard high-resistivity wafers and creation of grooves on its surfaces by usual microelectronics methods: reactive ion etching (RIE),

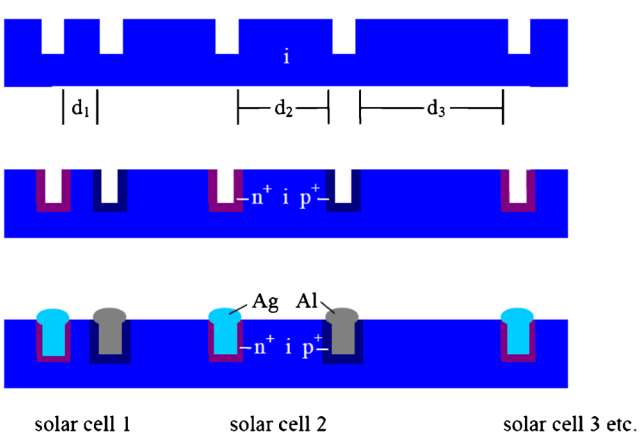

Fig. 11 Alternative laboratory implementation of PIN PV cells [17]

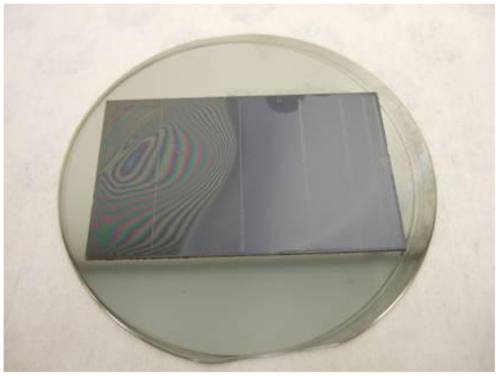

Fig. 12 Liquid etching of the silicon sample

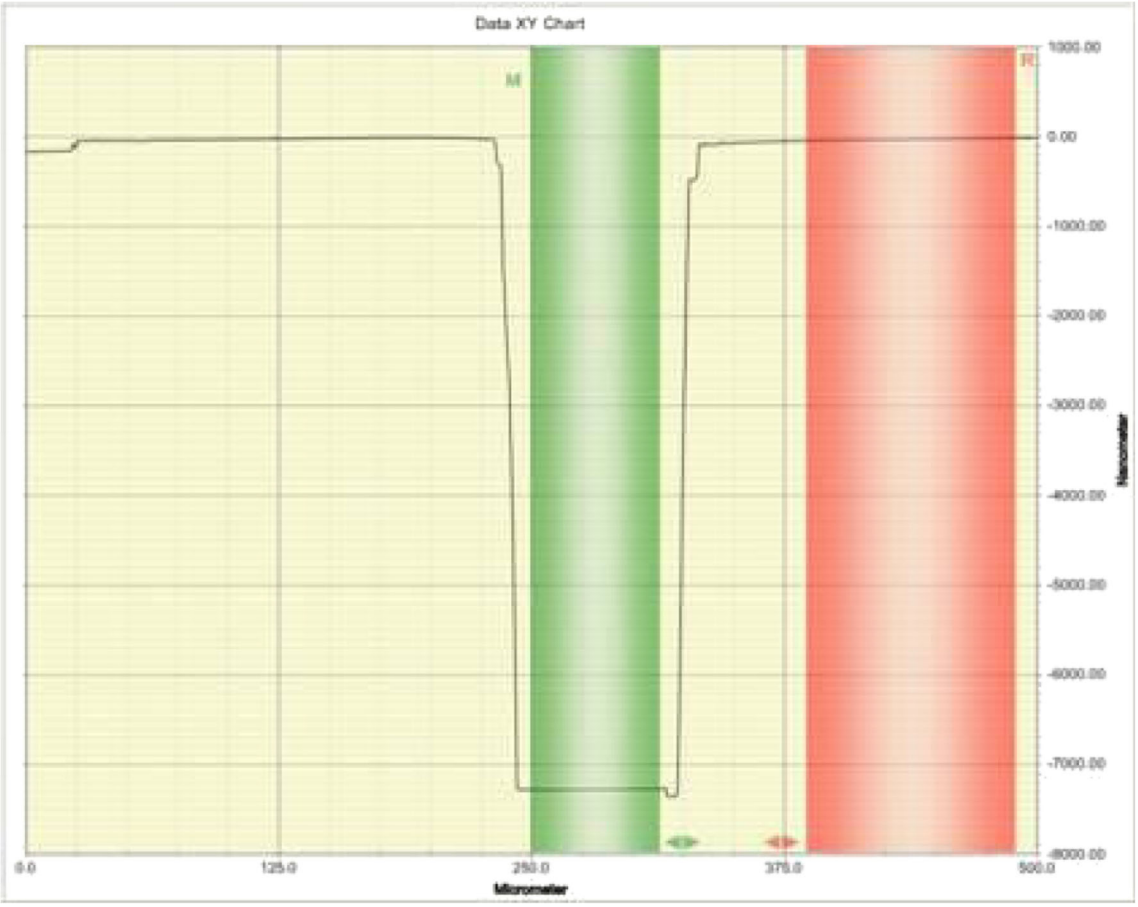

Fig. 13 15 min etch gave 7250 nm depth and 2170 nm broadening

brazing of metal pastes to dope the individual PV cells, etc. Figure 12 presents the laboratory etching of a silicon sample before RIE.

The next step was RIE to obtain the grooves of sufficient depth. Unfortunately, this process is not ready yet for our application. Figure 13 illustrates the profilometric results

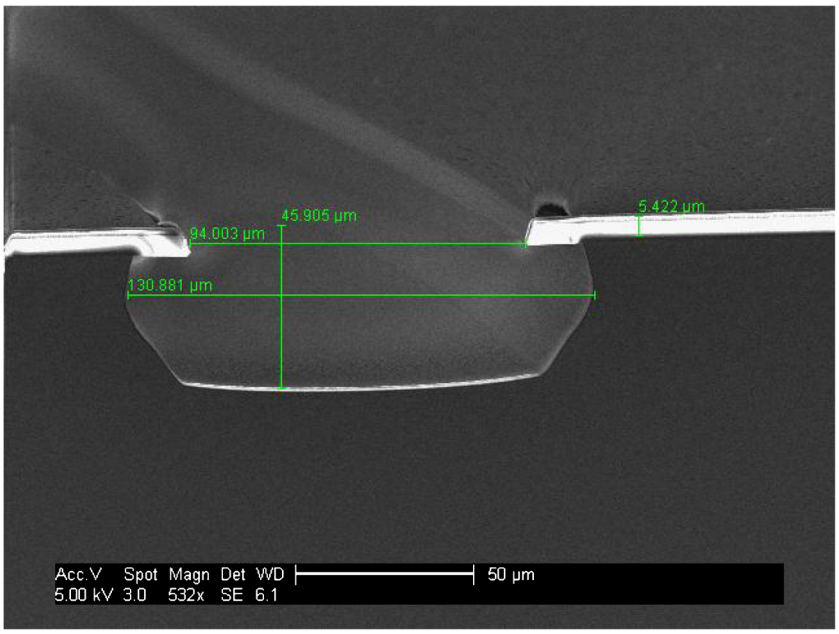

Fig. 14 The real picture of the prepared grooves

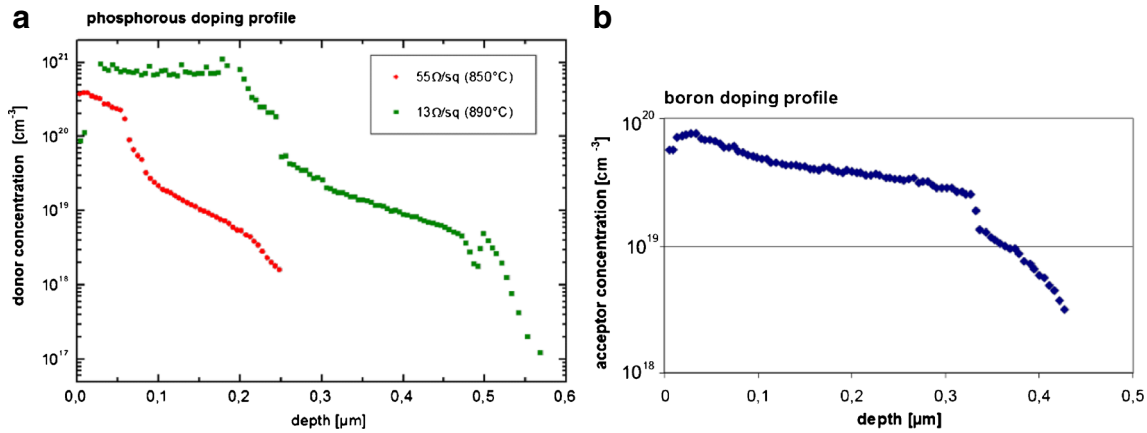

Fig. 15 Doping distribution on the edges of the grown PV cells: **a** Phosphorus; **b** Boron

and Fig. 14 shows the electron-microscopic photo of the grooving. The existing technology meets considerable difficulties in the practical implementation of the alternative technology, see Fig. 11.

Also, a metal paste brazing into the grooves cannot give a confident doping required by the PV cell properties. The highly doped regions at the edges of the samples were made by diffusion of boron and phosphorus, respectively. As it was not possible to measure the doping profiles on the real samples used for solar cell manufacturing, the respective profiles were measured on other wafers treated under the same conditions as the cells. Figure 15 shows the doping results obtained by electrochemical capacitive voltage measurements (ECV) after diffusion. As can be seen, only a small part of the walls of the groove is heavily doped. Therefore, we have an insufficient amount of charged carriers to build highly asymmetric junctions with an abrupt doping distribution enabling to create sufficient electric field. The contacts to the doped sides of the samples were made using metal-brazing pastes.

Anti-reflecting coating on the active surface of novel PV cells was deposited using plasma enhanced chemical vapor deposition (PECVD). The oxy-nitride films with thickness of approximately 70 nm were grown on the silicon samples on one side. The measured lifetime of the charged carriers under the anti-reflecting layers was of 5-10 ms, the measured minority carriers diffusion-length was of ∼4 mm. The efficiency of the best examined PV cells has reached $\eta = 11.9$ % and FF = 79.6 % for one-side illumination.

6 Summary and Discussion of the Results

A novel geometrical concept of a PIN-structure for PV applications, which enables direct bi-facial light irradiation, is projected to offer both excellent conversion efficiency and low cost fabrication by eliminating expensive fabrication steps, such as photolithography. The simulation results and first experimental results confirming our approach are summarized in Table 1. In comparison to conventional high-efficiency solar cells (e.g. HIT-cell, Sunpower cell), we expect to achieve comparable performance at an advantageous cost. But we expect an efficiency advantage over other cost-effective solutions for solar cells (e.g. SLIVER), which similarly employ narrow, bi-facial, edge contacted lateral solar cells, but not the PIN concept.

Table 1 Summary of results

Parameter	V_{oc}	I_{sc}	η	FF
This work (first experiments)	0.55 V	27.1 mA/cm^2	11.9 %	79.6 %
This work (projected by simulation)	0.755 V	54.0 mA/cm^2	28.0 %	82.3 %
SLIVER®solar cell [3]	0.686 V	37.1 mA/cm^2	19.4 %	81.0 %
Sanyo/Panasonic HIT solar cell [18]	0.750 V	41.8 mA/cm^2	24.7 %	83.2 %
UNSW/Sunpower solar cell [19]	0.721 V	40.5 mA/cm^2	24.2 %	82.9 %

7 Conclusions

Based on the simulation results and first measurements of practical implementations of our novel type of PV cells, we can conclude the following:

1 The lateral structure is preferable to the vertical one;
2 Despite the large width of the cells, the electric field generated in the semiconductor under illumination is sufficient for efficient separation of charged carriers;
3 The lateral construction provides full utilization of the active PV cell surfaces;
4 The lateral construction and right choice and orientation of the semiconductor crystal enables to minimize losses due to SRH and surface recombination mechanisms;
5 These PV cells can be used in a bi-facial illumination mode;
6 The maximal efficiency of these PV cells under bi-facial illumination can reach 28 %;
7 This lateral structure of the PV cell can be implemented into a manufacturing process.

References

1. Zakhidov RA (1994) Efficiency of solar cells. Appl Solar Energy 30(6):71–74
2. Burgers AR (1999) How to design optimal metallization patterns for solar cells. Prog Photovoltaics 7:457–461
3. Verlinden PJ, Blakers AW, Weber KJ, Babaei J, Everett V, Kerr MJ, Stuckings MF, Gordeev D, Stocks MJ (2006) Sliver® solar cells: a new thin-crystalline silicon photovoltaic technology. Sol Ener Mater Sol C 90:3422–3430
4. Minami T (2005) Transparent conducting oxide semiconductors for transparent electrodes. Semicond Sci Tech 20:S35–S44
5. Axelevitch A, Golan G (2007) Efficiency evaluation of multi-junction thin film solar cells, 26th IVS annual conference technical workshop, Israel, ES-04
6. Goetzberger A, Knobloch J, Voss B (1998) Crystalline Silicon Solar Cells. Wiley, Chichester
7. Axelevitch A, Golan G (2010) Efficiency analysis for multi-junction PV hetero-structures. In: Tanaka H, Yamashita K (eds) Photovoltaics: developments, applications and impact. Nova Science, New York, pp 213–247
8. Shah A (2010) Thin-film silicon solar cells. EPFL Press, Lausanne
9. Sze SM (1981) Physics of semiconductor devices. Wiley, New York
10. Shah A, Platz R, Keppner H (1995) Thin film silicon solar cells: a review and selected trends. Sol Ener Mater Sol C 38:501–520
11. Taur Y, Ning TH (2001) Fundamentals of modern VLSI devices. Cambridge University Press, Cambridge
12. Van Zeghbroeck B (2007) Principles of semiconductor devices, ecee.colorado.edu/~bart/book
13. Selberherr S (1984) Analysis and simulation of semiconductor devices. Springer-Verlag, Wien-New York
14. ATLAS framework integrated silicon device simulator (1998) Silvaco International
15. David Y, Golan G, Axelevitch A (2011) Simulation study of built-in electric field in lateral P-I-N silicon structure, 13th meeting on optical engineering and science in Israel –3rd OASIS, Israel, S5P1
16. Vitanov S, Vitanov P, Palankovski V (2008) Two-dimensional numerical optimization of MIS solar cell on N-type silicon, 23rd EUPVSEC 1743–1745
17. Golan G, Axelevitch A, Shavit R (2011) Photoelectric structure and method of manufacturing thereof, EP 2335290, H01L31/024
18. Taguchi M, Yano A, Tohoda S, Matsuyama K, Nakamura Y, Nishiwaki T, Fujita K, Maruyama E (2014) 24.7 % Record efficiency HIT solar cell on thin Silicon wafer. IEEE J Photovolt 4/1:96–99
19. Cousins PJ, Smith DD, Luan HC, Manning J, Dennis TD, Waldhauer A, Wilson KE, Harley G, Mulligan WP (2010) Generation 3: improved performance at lower cost. In: Proceedings 35th IEEE PVSC. Honolulu, pp 275–278